Journal of Mathematical Biology 77 (2018), 1689-1720

Periodic matrix models for seasonal dynamics of structured populations with application to a seabird population

J. M. Cushing[1] · **Shandelle M. Henson**[2]

Abstract For structured populations with an annual breeding season, life-stage interactions and behavioral tactics may occur on a faster time scale than that of population dynamics. Motivated by recent field studies of the effect of rising sea surface temperature (SST) on within-breeding-season behaviors in colonial seabirds, we formulate and analyze a general class of discrete-time matrix models designed to account for changes in behavioral tactics within the breeding season and their dynamic consequences at the population level across breeding seasons. As a specific example, we focus on egg cannibalism and the daily reproductive synchrony observed in seabirds. Using the model, we investigate circumstances under which these life history tactics can be beneficial or non-beneficial at the population level in light of the expected continued rise in SST. Using bifurcation theoretic techniques, we study the nature of non-extinction, seasonal cycles as a function of environmental resource availability as they are created upon destabilization of the extinction state. Of particular interest are backward bifurcations in that they typically create strong Allee effects in population models which, in turn, lead to the benefit of possible (initial condition dependent) survival in adverse environments. We find that positive density effects (component Allee effects) due to increased adult survival from cannibalism and the propensity of females to synchronize daily egg laying can produce a strong Allee effect due to a backward bifurcation.

Keywords Structured population dynamics, discrete-time population dynamics, periodically-forced matrix equations, periodic orbits, stability, bifurcations, seabird population dynamics, cannibalism, reproductive synchrony, animal behavior, Allee effect, tipping point

Mathematics MSC2010 subject classification 92D25, 92D40, 92D50, 37N25, 39A28, 39A60

1 Introduction

The Salish Sea, which consists of the connected marine waterways of British Columbia and Washington to the east and south of Vancouver Island, is an important region for breeding seabirds. Protection Island, in the south Salish Sea at the southeast end of the Strait of Juan de Fuca, is a particularly important breeding area, hosting over 70,000 seabirds [24]. More than 70% of the seabirds in Washington's coastal waterways nest on the island [10].

[1]Department of Mathematics and Interdisciplinary Program in Applied Mathematics, University of Arizona, 617 N Santa Rita, Tucson, AS 84721, USA

[2]Department of Mathematics and Department of Biology, Andrews University, 4260 and 4280 Administration Drive, Berrien Springs, MI 49104 USA

Glaucous-winged gulls (*Larus glaucescens*) breed in colonies along the west coast of North America from Oregon to Alaska. Over 2,400 pairs of glaucous-winged gulls nest in a colony on Violet Point (48°07'40"N, 122°55'3"W), a gravel spit on the southeast end of Protection Island [12]. In the spring, females lay two or three eggs in a clutch at approximately two-day intervals [33]. Parents take turns guarding the territory and incubating the eggs. The semi-precocious chicks hatch at about 27 days and fledge about six weeks later. Juvenile gulls become sexually mature in four years, often returning to their natal colony to nest [11]. The Protection Island colony does not have any ground predators, and the greatest sources of egg loss are due to bald eagle (*Haliaeetus leucocephalus*) predation and the cannibalization of eggs by conspecific neighbors [12],[13].

Average sea surface temperature (SST) in the Salish Sea has risen more than 1°C in the past few decades [31],[16]. Increases in SST often are associated with a lowered thermocline and lower plankton levels, leading to food deficits for marine birds [2],[28],[22],[30]. Gulls and other seabirds in the Salish Sea region are considered sentinels of environmental change [3],[18],[17].

In 2006-2015 our group carried out a study on the Violet Point colony to assess the effect of climate on reproductive and feeding tactics in glaucous-winged gulls [12],[13],[29]. We showed that:

- A 0.1 °C increase in SST was associated with a 10% increase in the odds that an egg was cannibalized by colony neighbors [12].
- During years of high SST, and hence high cannibalism rates [15], residents in dense parts of the colony synchronized clutch initiations on an every-other-day schedule [13].

Clutch initiation occurs when the first egg is laid in the nest. We found that the first egg was the most likely of the eggs in a clutch to be cannibalized and that it tended to be cannibalized on the day it was laid. We also found that first eggs laid synchronously with other first eggs were less likely to be cannibalized, suggesting that synchronous clutch initiation is advantageous in the presence of cannibalism [34].

The causal link between high SST and the two tactics of egg cannibalism and clutch-initiation synchrony probably is not direct, but likely is mediated by food resource level via the food web. Smith et al. [29] showed that SST in the early autumn before the breeding season was the best predictor of egg cannibalism and hatching success in glaucous-winged gulls. Decreased plankton abundance in early autumn can lead to fewer Pacific herring (*Clupea pallasii*) larvae in the spring, a major food resource for glaucous-winged gulls. This hypothesis is consistent with the fact that zooplankton abundance in October in the North Atlantic is the best predictor of the post-winter post-metamorphosis larvae of Atlantic herring (*C. harengus*) [1]. Thus, in this paper we consider SST a proxy for resource level.

We have considered several low-dimensional, proof-of-concept population and evolutionary dynamic models designed to study the effects of cannibalism on a population's reproductive timing, the nature of its dynamics, and its prospect for survival in a deteriorating environment [4], [14], [9], [32]. Using bifurcation theoretic techniques to study the bifurcation that occurs when the extinction equilibrium destabilizes, we have established several theoretical possibilities: a cannibalistic population can asymptotically persist in a deteriorated environment in which it would go extinct if it did not engage in cannibalism; reproductive synchrony can be a response to increased cannibalism activity; and cannibalism can be an evolutionarily stable strategy. Central to these analyses are backward bifurcations that lead to strong Allee effects [7], which imply initial condition dependent survival in a deteriorated environment and a "tipping" point for a catastrophic population collapse.

A discrepancy between the previously studied models and the population dynamics of the gull populations that motivated them is that those models assume juvenile maturation and adult reproductive synchrony are on commensurate time scales, whereas in gull populations the reproductive synchrony happens within a breeding season (on a daily time scale) and juveniles take several seasons (years) to reach maturity. Our purpose here is to derive and analyze a model that partially addresses this discrepancy by applying a within-breeding season projection matrix that is followed by an across-season projection matrix to account for over-winter mortality and maturation.

The gull model in this paper is an extension and generalization of one studied in [14]. It uses matrix model methodology to describe the breeding season dynamics of a juvenile-adult structured population coupled with a projection matrix to account for across season mortality and maturation. The model, which is derived and studied in Section 3, is an example of a general class of periodically-forced matrix models that is introduced and studied in Section 2. We show in Section 2 that an analysis of this class of models can be reduced to the analysis of a scalar map (one dimensional difference equation). Using bifurcation results for scalar maps, we obtain diagnostic quantities that determine the existence and stability properties of (seasonally) periodic solutions that bifurcate from the extinction equilibrium when it is destabilized by parameter manipulation. These results are then applied to the across-season gull model in Section 3 where we investigate the population dynamic consequences of cannibalism and reproductive synchrony as changes occur in the environmental resource availability.

2 A class of periodic matrix models

One use of periodic matrix models is to study seasonal variation in vital rates that occur over time intervals that are short in comparison to the seasonal cycle (for examples, see [5], [6] [20], [21], [23], [25], [26]). Here we consider a class of such models in which we separate the within breeding season vital rates from between breeding rates. Specifically, we consider the periodically-forced matrix model

$$\hat{x}\,(t+1) = P\,(t, \hat{x}(t))\,\hat{x}(t) \tag{1}$$

where $\hat{x}(t)$ is an m-dimensional demographic vector and the projection matrix $P\,(t, \hat{x})$ is defined by

$$P(t, \hat{x}) = \begin{cases} W(\hat{x}) & \text{for } t = 0, 1, \cdots, k-2 \\ A & \text{for } t = k-1 \end{cases} \tag{2}$$

extended periodically in t with integer period $k \geq 2$, i.e.

$$P\,(t+k, \hat{x}) = P\,(t, \hat{x}) \text{ for all } t \in Z$$

where $Z := \{0, 1, 2, 3, \cdots\}$. Let R_+ denote the non-negative real numbers, R_+^m denote the non-negative cone in m-dimensional Euclidean space R^m, and $\Omega \supset R_+^m$ denote an open set that contains R_+^m.

The matrix W accounts for the population dynamics during the breeding or reproductive season and we refer to it as the *within-season projection matrix*. The matrix A maps the population demographic vector from the end of a reproductive season to the start of the next reproductive season and we refer to it as the *across-season projection matrix*. The integer k is the *period of the reproductive cycle*. Note that $k-1$ is the length of the reproductive season. The unit of time during the reproductive period is chosen by the modeler in an appropriate and convenient

manner based on relevant life history stages of interest and on important reproductive events, competitive interactions, survival probabilities, and so on. The k^{th} time step taken across seasons is not necessarily the same unit. For example, during the reproductive season, the time unit might be a day while the across-season time unit might be several months.

We assume

A1. $A = [a_{ij}]$ and $W(\hat{x}) = [w_{ij}(\hat{x})]$ satisfy $a_{ij} \in R_+$, $\text{rank}(A) = 1$, and $w_{ij} : \Omega \to R^+$ is twice continuously differentiable for $1 \leq i, j \leq m$.

Our goal is to establish some theorems concerning the asymptotic dynamics of (1) by reducing the model equations to a scalar difference equation. Key to this reduction is the assumption in A1 that the matrix A has rank 1. This restriction is based on the assumption that the proportion of individuals in each demographic class is the same at the beginning of every reproductive season. We have in mind a scenario in which all individuals, regardless of their demographic class at the end of a reproductive season, will, if they survive to the start of the next reproductive season, mature and be reproductive adults at the start of the next reproductive season. If, in the model, there are several classes of adults (based, for example, on behavioral or physiological states), then the adults are distributed throughout these classes randomly with the same proportions (probabilities) at the beginning of every reproductive season.

Clearly the *extinction equilibrium* $\hat{x}(t) = \hat{0}$, $t \in Z$, is solution of (1). By a *nontrivial k-cycle* of (1) we mean a periodic solution of period k (i.e. $\hat{x}(t+k) = \hat{x}(t)$ for all t) that is not the extinction equilibrium. By a *non-extinction k-cycle* we mean a nontrivial k-cycle $\hat{x}(t)$ such that $\hat{x}(t) \in R_+^m$ for each t. If, on the other hand, k-cycle $\hat{x}(t)$ is not in R_+^m some all t, then we refer to $\hat{x}(t)$ as a *non-feasible k-cycle*.

The asymptotic dynamics of a k-periodically-forced difference equation can be analyzed by means of the $(k-1)^{st}$ composite equation (which is time autonomous). An equilibrium (or fixed point) of the composite equation corresponds to a k-periodic cycle of the original periodic equation (and vice versa). Moreover, the stability properties of the k-cycle are the same as the stability properties of the fixed point of the composite. Our main goal in this section is to show that under A1 the composite equation associated with (1)-(2) reduces to a scalar (one dimensional) difference equation and to draw some conclusions about the existence and stability of k-cycles from the scalar equation.

The demographic vector at the beginning of each season is $\hat{x}(nk)$ for $n \in Z$. By assumption A1, the range of the matrix A is one dimensional or, in other words, the columns of A are non-negative multiples of a vector

$$\hat{a} = \text{col}(a_i) \in R_+^m \backslash \{\hat{0}\}$$

which we can assume satisfies

$$\sum_{i=1}^{m} a_i = 1. \tag{3}$$

We can then write

$$A = [\ \nu_1 \hat{a} \quad \nu_2 \hat{a} \quad \cdots \quad \nu_m \hat{a}\ ], \quad \nu_j \geq 0 \text{ (not all 0)}. \tag{4}$$

By (2), $\hat{x}(nk) \in R_+^m$ lies in the range of A for $n \in Z \backslash \{0\}$ and therefore

$$\hat{x}(nk) = \alpha(n)\hat{a}, \quad n \in Z \backslash \{0\} \tag{5}$$

for a scalar $\alpha(n) \geq 0$. Regardless of the initial condition $\hat{x}(0)$, the vectors in the sequence $\hat{x}(k)$, $\hat{x}(2k)$, $\hat{x}(3k), \cdots$ – that is, the demographic population vector at the beginning of each season, after the first – are all multiples of $\hat{a}$. Therefore, in studying the model there is no loss in generality in assuming the initial condition $\hat{x}(0)$ is a multiple of $\hat{a}$:

$$\hat{x}(0) = \alpha\hat{a}. \tag{6}$$

From (3) follows

$$\alpha = \sum_{i=1}^{m} x_i(0)$$

and that α is the initial *total population size*.

Applying (1) for $t = 0, 1, 2, \ldots, k-1$ we obtain the sequence

$$\begin{aligned}
\hat{x}(0) &= \alpha\hat{a} \\
\hat{x}(1) &= W(\hat{x}(0))\,\alpha\hat{a} \\
\hat{x}(2) &= W(\hat{x}(1))\,W(\hat{x}(0))\,\alpha\hat{a} \\
\hat{x}(3) &= W(\hat{x}(2))\,W(\hat{x}(1))\,W(\hat{x}(0))\,\alpha\hat{a} \\
&\vdots \\
\hat{x}(i) &= \left(\prod_{i-1}^{t=0} W(\hat{x}(t))\right)\alpha\hat{a} \text{ for } i = 1, \cdots, k-1.
\end{aligned}$$

where

$$\prod_{i-1}^{t=0} W(\hat{x}(t)) := W(\hat{x}(i-1)) \cdots W(\hat{x}(1))\,W(\hat{x}(0)).$$

Define

$$Q(\alpha) := \prod_{k-2}^{t=0} W(\hat{x}(t)). \tag{7}$$

Then at the end of the first season, the population vector is $\hat{x}(k-1) = Q(\alpha)\,\alpha\hat{a}$ and at the beginning of the next season the population vector is

$$\hat{x}(k) = AQ(\alpha)\,\alpha\hat{a}.$$

The vector $AQ(\alpha)\,\hat{a}$ is a multiple of $\hat{a}$, say

$$AQ(\alpha)\,\hat{a} = r(\alpha)\,\hat{a}, \tag{8}$$

and thus

$$\hat{x}(k) = r(\alpha)\,\alpha\hat{a}.$$

The matrix model equation (1)-(2) maps an initial condition $\alpha\hat{a}$ at the beginning of a season to another multiple of $\hat{a}$, namely $r(\alpha)\,\alpha\hat{a}$, at the beginning of the next season, k steps later.

The sequence of demographic vectors at the beginning of the n^{th} season $\hat{x}(nk) = \alpha(n)\,\hat{a}$, which is given by the $(k-1)^{st}$ composite map of (1) with initial condition (6), satisfies the difference equation

$$\hat{x}((n+1)k) = r(\alpha(n))\,\hat{x}(nk)$$

where the sequence $\alpha(n)$ is given by the scalar recursion formula (difference equation)

$$\alpha(n+1) = r(\alpha(n))\,\alpha(n), \quad n \in Z. \tag{9}$$

Thus $r(\alpha)$ is a measure of the per season population growth rate. Note that (3) implies that $\alpha(n)$ is the *total population size at the beginning of each season.*

Since stability and instability properties of a period k orbit of a k periodically-forced map are equivalent to the stability and instability properties of the associated equilibrium (fixed point) of the $(k-1)^{st}$ composite map, we can study the existence and stability of k-cycles of the periodically-forced matrix model (1)-(2) by studying the existence and stability of equilibria of the (autonomous) scalar equation (9). The fixed point $\alpha = 0$ of (9) corresponds to the extinction equilibrium of model (1)-(2) and a positive fixed point corresponds to a non-extinction k-periodic cycle.

To study the scalar equation (9), we need to analyze the scalar function $r(\alpha)$ that defines it. From the across season projection matrix A, define the vector

$$\hat{\nu} := \mathrm{col}(\nu_i).$$

From (8) we obtain $\hat{a}^\tau A Q(\alpha)\hat{a} = \hat{a}^\tau r(\alpha)\hat{a}$ and hence

$$r(\alpha) = \frac{\hat{a}^\tau A Q(\alpha)\hat{a}}{\hat{a}^\tau \hat{a}}.$$

(The superscript τ denotes the matrix transpose.) Since

$$\hat{a}^\tau A = \begin{pmatrix} \nu_1\hat{a}^\tau\hat{a} & \nu_2\hat{a}^\tau\hat{a} & \cdots & \nu_m\hat{a}^\tau\hat{a} \end{pmatrix} = \hat{a}^\tau\hat{a}\;\hat{\nu}^\tau$$

we obtain a formula for the scalar map (9)

$$r(\alpha) = \hat{\nu}^\tau Q(\alpha)\hat{a}. \tag{10}$$

It follows from assumption A1 that $r(\alpha)$ is twice continuously differentiable on an open interval containing R^1_+ and satisfies $r(\alpha) \geq 0$ for $\alpha \geq 0$. Note that the *inherent (i.e. density-free) population growth rate* is

$$r(0) = \hat{\nu}^\tau Q(0)\hat{a} = \hat{\nu}^\tau W^{k-1}(0)\hat{a}. \tag{11}$$

The equilibrium $\alpha = 0$ of the difference equation (9) corresponds to the equilibrium $\hat{x} = \hat{0}$ of (1). A straightforward application of the linearization principle to the difference equation (9) shows that $\alpha = 0$ is locally asymptotically stable if $r(0) < 1$ and is unstable if $r(0) > 1$. It is not straightforward in general, however, to relate $r(0)$ explicitly to the model parameters appearing in the matrix equation (1). Nonetheless, by choosing a model parameter appearing in (1) and studying its effect on $r(0)$, we can derive some general facts about the existence and stability of non-extinction k-cycles as they depend on the chosen parameter.

2.1 Local bifurcation of non-extinction k-cycles

Let p be a parameter in the matrix W and write $W = W(p, \hat{x})$ and $P = P(p, \hat{x})$ in (1) and (2). The components of the composite matrix (7) also depend on p, which in turn means the population growth rate $r = r(p, \alpha)$ does as well. Accordingly we re-write (9) so as to indicate the dependence on p :

$$\alpha(n+1) = r(p, \alpha(n))\,\alpha(n), \quad n \in Z \tag{12}$$

where

$$r(p,\alpha) = \hat{\nu}^{\tau} Q(p,\alpha)\,\hat{a}.$$

The equation for a nontrivial equilibrium $\alpha \neq 0$ of (12) is

$$r(p,\alpha) = 1. \tag{13}$$

If α is an equilibrium of the scalar equation (12), then we call $(p,\alpha) \in R^2$ *an equilibrium pair*. If $\alpha > 0$ is an equilibrium, then we say (p,α) is a *positive equilibrium pair*. If $\alpha < 0$ we say (p,α) is a *negative* or *unfeasible equilibrium pair*. If α is a locally asymptotically stable (unstable) equilibrium of equation (12), then we say (p,α) is a *stable (unstable) equilibrium pair*.

Note that $(p,\alpha) = (p,0)$ is an *extinction equilibrium pair* of the scalar equation (12) for all values of p. If $\hat{x}(t)$ is the nontrivial k-cycle of the matrix model equation (1)-(2) that corresponds to an equilibrium pair (p,α), $\alpha \neq 0$, of (12), then we call the pair p and $\hat{x}(t)$ a *non-extinction* or *unfeasible k-cycle pair if* $\alpha > 0$ or $\alpha < 0$ respectively. Furthermore, if (p,α), $\alpha \neq 0$, is a stable (or unstable) equilibrium pair of (12), then the associated k-cycle pair p and $\hat{x}(t)$ of the matrix model equation (1)-(2) is stable (or unstable).

The central biological question of extinction or survival focuses on the extinction equilibrium pair $(p,0)$ of the scalar equation (12) and its stability properties, and therefore (by the linearization principle) on the sign of $r(p,0) - 1$. We focus on the destabilization of the extinction equilibrium by assuming that there is a value of $p = p_0$ at which $r(p,0) - 1$ changes sign. In the assumption below we use ∂ to denote partial differentiation and a super-script "0" to denote evaluation at $(p,\alpha) = (p_0,0)$, for example

$$\partial_{\alpha}^{0} r := \left.\frac{\partial r(p,\alpha)}{\partial \alpha}\right|_{(p,\alpha)=(p_0,0)} \quad \text{and} \quad \partial_{p}^{0} r := \left.\frac{\partial r(p,\alpha)}{\partial p}\right|_{(p,\alpha)=(p_0,0)}.$$

A2. Suppose p is a parameter appearing in the entries $w_{ij} = w_{ij}(p,x)$ of the matrix $W = W(p,x)$ in A1. Assume $w_{ij}(p,x)$ are twice continuously differentiable in p on an open interval containing a parameter value p_0 such that $r(p_0,0) = 1$ and $\partial_p^0 r \neq 0$. Furthermore, assume $\partial_{\alpha}^{0} r \neq 0$.

By applying Lemma 1 in the Appendix to the scalar difference equation (12), we obtain the following Theorem 1, which describes the bifurcation alternatives for the corresponding non-extinction k-cycle pairs $(p,\hat{x}(n))$ of matrix equation (1)-(2) at the parameter value $p = p_0$ in A2 where the extinction equilibrium destabilizes. The theorem assumes $\partial_p^0 r > 0$ in A2. If $\partial_p^0 r < 0$ in A2, then the results described in Theorem 1 remain valid, but with inequalities reversed.

Theorem 1 *Assume A1, A2 and that* $\partial_p^0 r > 0$. *The extinction equilibrium pairs* $(p,\hat{0})$ *are locally asymptotically stable for* $p \lessapprox p_0$ *and unstable for* $p \gtrapprox p_0$.[3] *There exists a continuum of nontrivial k-cycle solution pairs* $(p,\hat{x}(n))$ *of the matrix difference equation (1)-(2) that (transcritically) bifurcates from the extinction pair* $(p_0,\hat{0})$.

(a) If $\partial_{\alpha}^{0} r < 0$ *then the bifurcating k-cycle pairs* $(p,\hat{x}(n))$ *are locally asymptotically stable, non-extinction k-cycle pairs for* $p \gtrapprox p_0$, *but are non-feasible k-cycles pairs for* $p \lessapprox p_0$. *In this case, we say a* ***forward, stable bifurcation*** *occurs at* $p = p_0$.

(b) If $\partial_{\alpha}^{0} r > 0$ *then the bifurcating k-cycle nontrivial pairs* $(p,\hat{x}(n))$ *are unstable, non-extinction k-cycles for* $p \lessapprox p_0$, *but are non-feasible k-cycles pairs for* $p \gtrapprox p_0$. *In this case, we say a* ***backward, unstable bifurcation*** *occurs at* $p = p_0$.

[3] By $a \lessapprox b$ is meant both $a < b$ and $|a-b|$ is small. Similarly, $a \gtrapprox b$ means both $a > b$ and $|a-b|$ is small.

A pair $(p, \alpha) \in R^2$ is a nontrivial equilibrium pair (i.e. $\alpha \neq 0$) of the scalar equation (12) if and only if it satisfies the equation (13). Thus, a geometric way to represent positive equilibrium pairs is to plot the graph defined by this equation, i.e. to plot the set of points

$$G := \{(p, \alpha) : r(p, \alpha) = 1\},$$

in the (p, α)-plane. We are particularly interested in the positive equilibrium pairs, represented by the graph

$$G_+ = \{(p, \alpha) \in G : \alpha > 0\}.$$

Given the correspondence between the equilibrium pairs (p, α) of the scalar equation (12) and the k-cycles of the matrix equation (1) with (2), the graph G_+ also describes the non-extinction k-cycles of the matrix equation. Since $(p_0, 0)$ also satisfies equation (13), the graph G intersects the graph of the extinction equilibrium pairs (which is the p-axis in the (p, α)-plane) at this point. The intersection described in Theorem 1 is a transcritical bifurcation at $(p_0, 0)$ with a concomitant exchange of stability between branches [19].

Cartoon graphs illustrating the bifurcation scenarios described in Theorem 1 appear as the first row of plots in Figure 1. If in A2 we have $\partial_p^0 r < 0$ instead, then the inequalities in Theorem 1 are reversed and we get bifurcation alternatives also shown in the second row of plots in Figure 1. In either case, notice that the *direction of bifurcation* determines the stability of the bifurcating equilibrium pairs.

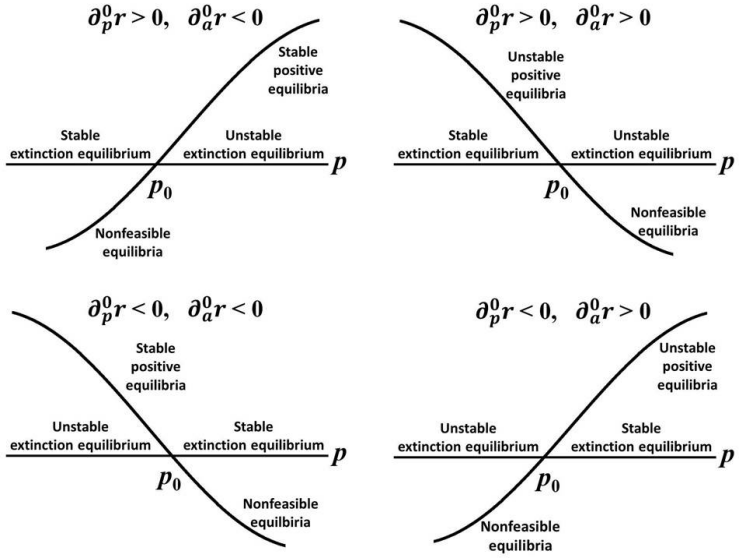

Figure 1. The four bifurcation alternatives for the scalar equation (12) that plot equilibrium pairs (p, α) in the (p, α)-plane in a neighborhood of a bifurcation point $(p_0, 0)$. The horizontal line is the graph of the extinction equilibrium pairs $(p, 0)$ and the intersecting curves are the graphs of G. Each pair (p, α) corresponds to a k-cycle of the matrix equation (1) with (2) so that the first row these plots schematically describe the bifurcation of the k-cycles as given in Theorem 1. If $\partial_p^0 r < 0$ replaces $\partial_p^0 r > 0$ in A2, then the bifurcation alternatives are shown in the second row of plots.

By Theorem 1 we see that near the bifurcation point $(p_0, \hat{0})$ the bifurcating non-extinction k-cycles guaranteed by Theorem 1 are stable if $\partial_\alpha^0 r < 0$ and unstable if $\partial_\alpha^0 r > 0$, regardless of the sign of $\partial_p^0 r$. A proof of the following corollary is given in the Appendix.

Corollary 1 *Assume A1 and A2. The quantity $\partial_\alpha^0 r$ is a linear combination, constructed with non-negative coefficients, of the derivatives $\partial_{x_l}^0 w_{ij}$ of the entries in the within-season matrix W taken with respect to entries x_l of $\hat{x}$ (and evaluated at the bifurcation point $\hat{x} = \hat{0}$, $p = p_0$).*

The partial derivatives $\partial_{x_l}^0 w_{ij}$ measure the effects that changes in low level, class specific densities have on the entry w_{ij} in the within-season projection matrix W. We say a *negative density effect occurs at low population densities* if $\partial_{x_l}^0 w_{ij} < 0$, i.e. when increased low-level density x_l decreases w_{ij}. We say a *positive density effect occurs at low population densities* (which is sometimes called a *component Allee effect*) if $\partial_{x_l}^0 w_{ij} > 0$, i.e. when increased low-level density x_l increases w_{ij}.

Corollary 1 implies, in conjunction with Theorem 1, that the bifurcation of stable k-cycles occurs when negative density effects are predominant at low population densities (in the sense that $\partial_\alpha^0 r < 0$) whereas the bifurcation of unstable, non-extinction k-cycles occurs if positive density effects are predominant at low population densities (in the sense that $\partial_\alpha^0 r > 0$).

2.2 k-cycles outside a neighborhood of the bifurcation point

Theorem 1 describes the properties of the bifurcating continuum of non-extinction k-cycles $(p, \hat{x}(n))$ in a neighborhood of the bifurcation point $(p, \hat{0})$, which we will call the *primary bifurcation point*. Because non-extinction k-cycles of the matrix equation (1)-(2) correspond to positive equilibria of a scalar equation (12), it is possible to investigate the stability properties of k-cycles that are not necessarily near the bifurcation by investigating the geometry of the graph G_+ in the (p, α)-plane.

First of all, we recall that it is well-known for scalar difference equations that positive equilibrium pairs (p, α) can suffer secondary bifurcations, where their stability properties change, outside of a neighborhood of the primary bifurcation point at $(p_0, 0)$. The famous period-doubling cascade to chaos for scalar equations for which the graph of $r(\alpha) a$ has a "hump", such as the case for the exponential (Ricker) nonlinearity $\exp(-c\alpha)\alpha$, is perhaps the most well-known example. The stability properties of positive equilibrium pairs outside a neighborhood of the bifurcation point depends crucially on the properties of the nonlinearities in α appearing in $r(p, \alpha)$ (i.e. the nonlinearities in $\hat{x}$ present in the entries w_{ij} of the seasonal projection matrix matrix W). Nonetheless, as we will see, some general stability and instability criteria are available for equilibrium pairs lying on certain segments of the graph C_+.

By the linearization principle, an equilibrium pair (p, α) of the scalar equation (12) is (locally asymptotically) stable if $|\partial_\alpha (r(p, \alpha)\alpha)| < 1$ and is unstable if $|\partial_\alpha (r(p, \alpha)\alpha)| > 1$. At an equilibrium pair, the derivative

$$\partial_\alpha (r(p, \alpha)\alpha) = r(p, \alpha) + \alpha \partial_\alpha r(p, \alpha)$$

becomes

$$\partial_\alpha (r(p, \alpha)\alpha) = 1 + \alpha \partial_\alpha r(p, \alpha)$$

From this we see that $\partial_\alpha (r(p, \alpha)\alpha) > 1$ at a positive equilibrium pair (p, α) if $\partial_\alpha r(p, \alpha) > 0$, in which case the equilibrium pair is unstable. On the other hand, if $\partial_\alpha r(p, \alpha) < 0$ then the equilibrium pair is stable provided $-2 < \alpha \partial_\alpha r(p, \alpha) < 0$. Let us say that an equilibrium pair (p, α) is a *critical equilibrium pair* if $\partial_\alpha r(p, \alpha) = 0$.

Theorem 2 *Assume A1 and A2. Let (p, α) be the positive equilibrium pair associated with a non-extinction k-cycle of (1)-(2).*

(a) The non-extinction k-cycle is unstable if $\partial_\alpha r\,(p, \alpha) > 0$. Geometrically this means the k-cycle is unstable if (p, α) lies on a strictly decreasing segment of the graph G_+ if $\partial_p r\,(p, \alpha) > 0$ (or on a monotone increasing segment of G_+ if $\partial_p r\,(p, \alpha) < 0$).

(b) The non-extinction k-cycle is (locally asymptotically) stable if $-2 < \alpha\partial_\alpha r\,(p, \alpha) < 0$. Geometrically this means the k-cycle is stable if (p, α) lies near a critical equilibrium pair on an increasing segment of G_+ when $\partial_p r\,(p, \alpha) > 0$ (or on a decreasing segment of G_+ if $\partial_p r\,(p, \alpha) < 0$).

Proof. An application of the implicit function theorem to the equilibrium equation (13) shows that the graph G_+ in a neighborhood of the equilibrium pair (p, α) is a smooth curve given by a twice continuously differentiable function $p = \zeta\,(a)$. An implicit differentiation of $r\,(\zeta\,(\alpha)\,, \alpha) = 1$ with respect to α yields $\partial_p r\zeta' + \partial_\alpha r = 0$ and $\zeta' = -\partial_\alpha r/\partial_p r \neq 0$. The sign of ζ' is the opposite of the sign of $\partial_\alpha r/\partial_p r$ from which follow the geometric assertions in (a) and (b) concerning the monotonicity of G_+ at the positive equilibrium pair (p, α). ■

The graph of G_+ in the (p, α)-plane is the reflection through the line $\alpha = p$ of the graph in the (α, p)-plane. A local extremum of G_+ in the (p, α)-plane is a critical equilibrium pair, and it is a *tangent (saddle-node or blue-sky) bifurcation point* in the (p, α)-plane, as illustrated in Figure 2. Figure 2 geometrically summarizes the results of Theorem 2 in the case $\partial_p r\,(p, \alpha) > 0$ for all (p, α), which is the most commonly occurring case in applications.

A common and important scenario that often (usually) results in population models with a backward bifurcation is illustrated in Figure 2B when $\partial_p r > 0$. As we observed, a backward bifurcation occurs because of dominant *positive* density effects at *low* population densities (component Allee effects). However, most population models assume that *negative* density effects are dominant at *high* population densities. This model assumption provides density regulation against unbounded population growth and it means $r\,(p, \alpha)$ decreases for increases in large values of α, i.e. $\partial_\alpha r\,(p, \alpha) < 0$ for large α. As we follow the non-extinction equilibrium pairs (p, α) backward, to the left from the bifurcation point $(p_0, 0)$ in Figure 2B, the component p decreases and the component α increases. The equality $r\,(p, \alpha) = 1$ is maintained, near the bifurcation point, by $\partial_p r > 0$ and $\partial_\alpha r > 0$. However, as the α component increases to the point that negative density effects come into play, so that $\partial_\alpha r < 0$, then in order to maintain the equality $r\,(p, \alpha) = 1$, the p component of the equilibrium pair must increase (since $\partial_p r > 0$). This implies the graph G_+ "turns around" as shown in Figure 2B, which in turn results in a stabilization of the equilibrium pair. This scenario therefore results in *multiple attractors, one of which is the extinction equilibrium and another of which is a positive equilibrium pair.* This scenario is called a *strong Allee effect* and it is a hallmark of backward bifurcations in population models [7], [8].

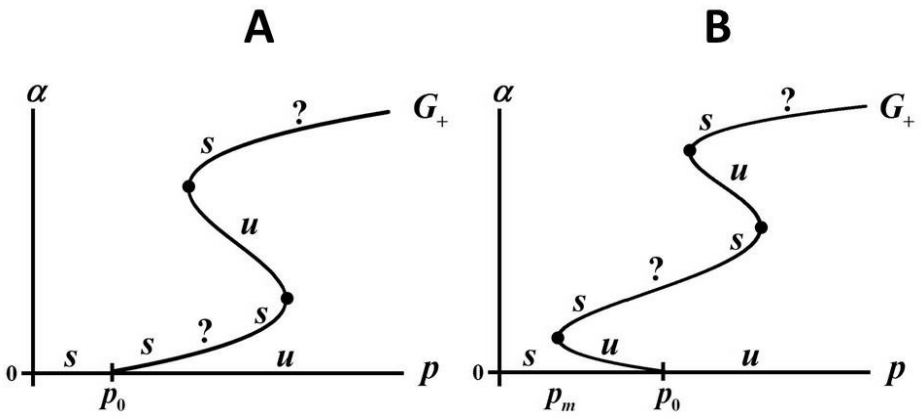

Figure 2. These plots summarize the relationship between the geometry of the graph G_+ of positive equilibrium pairs of the scalar difference equation (12) and their stability and instability when $\partial_p r > 0$ for all (p, α). By Theorem 2(a) equilibrium pairs located anywhere on decreasing segments of G_+ are unstable and those located on increasing segments near the critical equilibrium pairs denoted by solid circles are (locally asymptotically) stable. The question marks emphasize that, by Theorem 2(b), stability on increasing segments is guaranteed in general only at points near the critical points (tangent bifurcation points of the scalar equation (12)) and near the primary transcritical bifurcation point $(p_0, 0)$.

The significance of a strong Allee effect of this kind in population models is that it provides for survival for parameter values when $r(p, 0) < 1$ even though the extinction state is stable. Survival in this case is initial condition dependent, of course, since the initial population must lie outside the basin of attraction of the extinction equilibrium.

As an example illustrating Theorems 1 and 2, consider a matrix model (1)-(2) with a two dimensional demographic vector of juveniles x_1 and adults x_2 and matrices

$$W(x_1, x_2) = \begin{pmatrix} s_1\sigma(x_2) & b\varphi(x_2) \\ 0 & s_2 \end{pmatrix}, \qquad A = \begin{pmatrix} 0 & 0 \\ \nu_1 & \nu_2 \end{pmatrix}$$

where

$$0 < s_1, s_2 < 1,\ b > 0$$

$$0 \le \nu_i < 1 \text{ and } \nu_i \text{ are not both } 0$$

and where σ and φ are twice continuously differentiable on an open half line containing R_+ satisfying

$$\sigma(0) = \varphi(0) = 1,\ \varphi(x) > 0 \text{ and } 0 < s_1\sigma(x) < 1 \text{ on } R_+.$$

Here $b\varphi(x_2)$ juveniles are produced per time unit per adult, and $s_1\sigma(x_2)$ and s_2 are the per unit time survival probabilities of juveniles and adults respectively. The probabilities that a juvenile and an adult survives from the end of one season to the start of the next season are ν_1 and ν_2

respectively. The normalization of σ and φ at $x_2 = 0$ means that b and s_i are the density-free (or inherent) fertility and survival rates, respectively. In this example we assume adult fertility is regulated by adult population density in a negative way, i.e.

$$\varphi'(x) < 0,\ x \geq 0.$$

We also assume that adult density effects on juvenile survival is a positive one (a component Allee effect), which could be attributed, for example, to protection of juveniles by adults, so that

$$\sigma'(x) > 0,\ x \geq 0.$$

We use $p = b$ as the bifurcation parameter.

From A we have

$$\hat{a} = \begin{pmatrix} 0 \\ 1 \end{pmatrix}.$$

We calculate $Q(\alpha)$ from (7) by induction and obtain

$$Q(p,\alpha) = \begin{pmatrix} s_1\sigma(\alpha) & b\varphi(\alpha) \\ 0 & s_2 \end{pmatrix} \text{ if } k = 2$$

$$Q(p,\alpha) = \begin{pmatrix} s_1^{k-1}\prod_{i=0}^{k-2}\sigma\left(s_2^i\alpha\right) & p\left(\sum_{i=0}^{k-3}s_1^{k-2-i}s_2^i\varphi\left(s_2^i\alpha\right)\prod_{j=i+1}^{k-2}\sigma\left(s_2^j\alpha\right) + s_2^{k-2}\varphi\left(s_2^{k-2}\alpha\right)\right) \\ 0 & s_2^{k-1} \end{pmatrix} \text{ if } k \geq 3.$$

From these, used in (10), we find that

$$r(p,\alpha) = \begin{cases} \nu_1 p\varphi(\alpha) + \nu_2 s_2 & \text{if } k = 2 \\ \nu_1 p\psi(\alpha) + \nu_2 s_2^{k-1} & \text{if } k \geq 3 \end{cases}$$

in which we have defined

$$\psi(\alpha) := \sum_{i=0}^{k-3}\left(s_1^{k-2-i}s_2^i\varphi\left(s_2^i\alpha\right)\prod_{j=i+1}^{k-2}\sigma\left(s_2^j\alpha\right)\right) + s_2^{k-2}\varphi\left(s_2^{k-2}\alpha\right) > 0. \tag{14}$$

From

$$r(p,0) = \begin{cases} \nu_1 p + \nu_2 s_2 & \text{if } k = 2 \\ \nu_1 p\psi(0) + \nu_2 s_2^{k-1} & \text{if } k \geq 3 \end{cases}$$

$$0 < \psi(0) = \sum_{i=0}^{k-2}s_1^{k-2-i}s_2^i = \begin{cases} \frac{s_2^{k-1}-s_1^{k-1}}{s_2-s_1} & \text{if } \ s_2 \neq s_1 \\ (k-1)\,s_1^{k-2} & \text{if } \ s_2 = s_1 \end{cases}$$

we obtain the bifurcation point (where $r(p,0) = 1$ and the extinction equilibrium destabilizes) for $p = b$ is

$$p_0 = \begin{cases} (1-\nu_2 s_2)/\nu_1 & \text{if } k = 2 \\ \left(1-\nu_2 s_2^{k-1}\right)/\nu_1\psi(0) & \text{if } k \geq 3 \end{cases}.$$

Note that

$$0 < \partial_p r(p,\alpha) = \begin{cases} \nu_1\varphi(\alpha) & \text{if } k = 2 \\ \nu_1\psi(\alpha) & \text{if } k \geq 3 \end{cases}.$$

and hence by Theorem 1 the direction of bifurcation and the stability of bifurcating k-cycles at $p = p_0$ is determined by the sign of

$$\partial_\alpha^0 r = \begin{cases} \nu_1 p_0 \varphi'(0) & \text{if } k = 2 \\ \nu_1 p_0 \psi'(0) & \text{if } k \geq 3 \end{cases}.$$

We conclude that a forward and stable bifurcation occurs when $k = 2$ and when $\psi'(0) < 0$ for $k \geq 3$. The bifurcation is backward and unstable when $\psi'(0) > 0$ for $k \geq 3$. A calculation from (14 using the product and chain rules shows $\psi'(0)$ is a linear combination of $\varphi'(0)$ and $\sigma'(0)$:

$$\begin{aligned} \psi'(0) &= \sum_{i=0}^{k-3} s_1^{k-2-i} s_2^{2i} \varphi'(0) + \sum_{i=0}^{k-3} s_1^{k-2-i} s_2^i \sum_{j=i+1}^{k-2} s_2^j \sigma'(0) + s_2^{2(k-2)} \varphi'(0) \\ &= \varphi'(0) \sum_{i=0}^{k-2} s_1^{k-2-i} s_2^{2i} + \sigma'(0) \sum_{i=0}^{k-3} s_1^{k-2-i} s_2^{2i} \sum_{j=i+1}^{k-2} s_2^{j-i}. \end{aligned}$$

This formula quantifies the magnitude of the positive density effect on juvenile survival $\sigma'(0)$ (relative to the negative density effect on adult fertility $\varphi'(0)$) in order that a backward bifurcation occurs, i.e. in order for for $\psi'(0) > 0$.

3 A seabird population model

Motivated by the observations and studies of marine birds described in Section 1, we construct a matrix model of the type (1)-(2) designed to investigate the population dynamic consequences of the individual behavioral tactics of egg cannibalism and reproductive synchronization that occur during each breeding season. We specify four classes of individuals, which we call *eggs*, *juveniles*, *reproductively active female adults*, and *non-reproductively active female adults*. The number of *eggs*, denoted $x_1(t)$, is the number of eggs laid on day t. A *juvenile* in this model is either an egg older than one day or a chick, and the number of juveniles at time t is denoted $x_2(t)$. The individual ovulation cycle for each adult female gull is about two days, and each female lays an egg approximately every other day. The number of *reproductively active adults*, $x_3(t)$, is the number of female adults that are in the first day of the avian hormone cycle on day t. These are the females that lay an egg on day t. The number of *non-reproductively active adults*, $x_4(t)$, is the number of female adults in the second day, or non-reproductive day, of the hormone cycle on day t; these females do not lay an egg on day t. After the breeding season of $k-1$ days, a between-season mortality is applied. All surviving eggs and chicks are assumed to mature during the between-season interval, after which the females are placed into either class x_3 or class x_4 at the start of the following season.

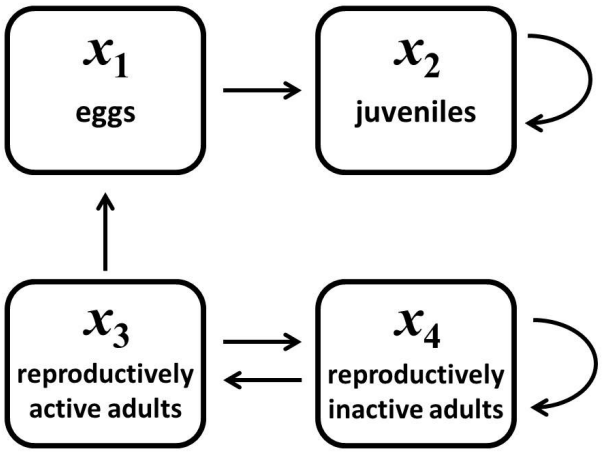

Figure 3 A compartmental diagram for the within-season dynamics described by $W(x)$ .The time step is one day.

The model is a periodically-forced, nonlinear, four-dimensional map

$$\hat{x}(t+1) = P(t, \hat{x}(t))\,\hat{x}(t) \tag{15}$$

where

$$\hat{x} = \begin{pmatrix} x_1 \\ x_2 \\ x_3 \\ x_4 \end{pmatrix} = \begin{pmatrix} \text{eggs} \\ \text{juveniles} \\ \text{reproductively active adults} \\ \text{reproductively inactive adults} \end{pmatrix}$$

is the vector of life stages, the time step is one day, and the k-periodic projection matrix $P(t, \hat{x})$ is defined as follows. The within-season projection matrix derived from the diagram in Figure 3 has the form

$$W(\hat{x}) = \begin{pmatrix} 0 & 0 & b\beta(\hat{x}) & 0 \\ s_1\sigma_1(\hat{x}) & s_2\sigma_2(\hat{x}) & 0 & 0 \\ 0 & 0 & 0 & s_4\sigma_4(\hat{x})\,g(x_3) \\ 0 & 0 & s_3\sigma_3(\hat{x}) & s_4\sigma_4(\hat{x})\,(1-g(x_3)) \end{pmatrix}. \tag{16}$$

The term $b\beta(\hat{x})$ is the number of eggs produced per reproductively active female. The terms $s_i\sigma_i(\hat{x})$ are the fractions of i-class individuals that survive one time unit (day). Note that a surviving class 1 individual (egg) moves to the juvenile class 2 and a surviving class 3 (reproductively active) individual moves to the reproductively inactive class 4 (because of the reproductive refractory period). A surviving class 4 (non-reproductively active) individual moves to class 3, i.e. becomes reproductively active, with probability g and otherwise remains in class 4. Note that we have assumed this fraction $g = g(x_3)$ depends only on the number of reproductively active females x_3.

All of the density dependent terms are assumed twice continuously differentiable on an open set Ω containing the non-negative cone R^4_+ and satisfy

$$b\beta(\hat{x}) \geq 0, \quad 0 \leq s_i\sigma_i(\hat{x}) < 1, \quad 0 < g(x_3) \leq 1$$

$$\beta(\hat{0}) = 1, \quad \sigma_i(\hat{0}) = 1, \quad g(0) = 1$$

for all $\hat{x} \in \Omega$. We assume only adult density regulation of reproduction by setting

$$\beta(\hat{x}) = \varphi(c_{\varphi 3} x_3 + c_{\varphi 4} x_4)$$

where φ is a decreasing function of a weighted total adult population size $c_{\varphi 3} x_3 + c_{\varphi 4} x_4$, $c_{\varphi i} \geq 0$ (not both 0):

$$\varphi'(z) := \frac{d\varphi}{dz} < 0.$$

We design the remaining entries in the projection matrix so as to incorporate adult-on-egg cannibalism and for a capability for females to reproductively synchronize. We assume egg survival is subject to adult cannibalism in the following way. Let $\pi_i(x_1, x_i) x_i$ denote the probability a egg is cannibalized in the presence of x_i adults of class $i = 3, 4$ so that

$$\sigma_1(\hat{x}) = \prod_{i=3}^{4} (1 - \pi_i(x_1, x_i) x_i)$$

where

$$0 \leq \pi_i(x_1, x_i) x_i \leq 1$$

for all $\hat{x} \in \Omega$. The dependence of π_i on x_1 allows for a victim saturation effect on cannibals in analogy with the familiar predator saturation effect of prey on predators. Thus, we assume

$$\partial_{x_1} \pi_i := \frac{\partial \pi_i}{\partial x_1} \leq 0, \quad \partial_{x_i} \pi_i := \frac{\partial \pi_i}{\partial x_i} \geq 0$$

We also assume juvenile survival is density independent

$$\sigma_2(\hat{x}) \equiv 1,$$

and that adult survival is increased by cannibalism resources so that

$$\sigma_i(\hat{x}) = \sigma_i(\pi_i(x_1, x_i) x_1), \quad i = 3 \text{ and } 4$$

where σ_i is an increasing function of the number of eggs cannibalized $\pi_i(x_1, x_i) x_1$ by an individual i-class adult, with

$$\sigma_i'(z) := \frac{d\sigma_i(z)}{dz} > 0.$$

Finally we assume

$$g'(x_3) := \frac{dg}{dx_3} < 0.$$

so that a larger active adult density on any given day decreases the probability that inactive adults become active the next day. We refer to g as the *synchrony propensity term.*

To account for a trade-off between environmental resource availability and cannibalism activity, we let $\rho > 0$ denote the amount of available environmental resource and assume $b = b(\rho)$ and $\pi_j = \pi_j(\rho, x_1, x_j)$ are functions of ρ satisfying

$$b'(\rho) > 0, \quad \partial_\rho \pi_j(\rho, x_1, x_j) < 0.$$

We also assume that in the absence of the environmental resource. reproduction ceases, so that

$$b\left(0\right)=0.$$

In a more general model, the inherent survivorships s_i could also depend on ρ, but we will investigate only the case here when they are independent of ρ. We choose

$$p=\rho$$

as the bifurcation parameter in order to study the effect of changing environmental resource availability.

Under these assumptions, the projection matrix (16) becomes

$$W\left(\rho,\hat{x}\right)=\begin{pmatrix}0 & 0 & w_{13}\left(\rho,\hat{x}\right) & 0\\ w_{21}\left(\rho,\hat{x}\right) & w_{22}\left(\rho,\hat{x}\right) & 0 & 0\\ 0 & 0 & 0 & w_{34}\left(\rho,\hat{x}\right)\\ 0 & 0 & w_{43}\left(\rho,\hat{x}\right) & w_{44}\left(\rho,\hat{x}\right)\end{pmatrix}. \tag{17}$$

$$w_{13}\left(\rho,\hat{x}\right)=b\left(\rho\right)\varphi\left(c_{\varphi_3}x_3+c_{\varphi_4}x_4\right) \tag{18a}$$

$$w_{21}\left(\rho,\hat{x}\right)=s_1\left(1-\pi_3\left(\rho,x_1,x_3\right)x_3\right)\left(1-\pi_4\left(\rho,x_1,x_4\right)x_4\right),\ w_{22}\left(\rho,\hat{x}\right)=s_2 \tag{18b}$$

$$w_{34}\left(\rho,\hat{x}\right)=s_4\sigma_4\left(\pi_4\left(\rho,x_1,x_4\right)x_1\right)g\left(x_3\right) \tag{18c}$$

$$w_{43}\left(\rho,\hat{x}\right)=s_3\sigma_3\left(\pi_3\left(\rho,x_1,x_3\right)x_1\right),\ w_{44}\left(\rho,\hat{x}\right)=s_4\sigma_4\left(\pi_4\left(\rho,x_1,x_4\right)x_1\right)\left(1-g(x_3)\right) \tag{18d}$$

We now turn our attention to the across season projection matrix A. A compromise we will make in the model considered here is that immature individuals reach maturation after one season (in contrast to the four seasons typical of the glaucous winged gull).

We assume the census takes place at the end of each day, during which the nonlinear effects take place. After the final day of the breeding season, there is a demographic vector with individuals present in each of the four classes. During the across-season time interval, all surviving non-adult individuals mature and we assume a (density independent) probability of survival $\nu_i\geq 0$ for each of the population classes during this time interval (which includes over-winter survival). On the first day of the next breeding season, the population consequently consists of adults only, a fraction ν which we assume is reproductively active on that first day. Thus, the across-season projection matrix is

$$A=\begin{pmatrix}0 & 0 & 0 & 0\\ 0 & 0 & 0 & 0\\ \nu_1\nu & \nu_2\nu & \nu_3\nu & \nu_4\nu\\ \nu_1(1-\nu) & \nu_2(1-\nu) & \nu_3(1-\nu) & \nu_4(1-\nu)\end{pmatrix}. \tag{19}$$

The general theory and results in Section 2 apply to this model (17)-(19) with

$$\hat{a}=\begin{pmatrix}0\\ 0\\ \nu\\ 1-\nu\end{pmatrix},\qquad \hat{\nu}=\begin{pmatrix}\nu_1\\ \nu_2\\ \nu_3\\ \nu_4\end{pmatrix}. \tag{20}$$

As is done in the general model in Section 2, we consider initial conditions of the form

$$\hat{x} = \alpha \begin{pmatrix} 0 \\ 0 \\ \nu \\ 1-\nu \end{pmatrix}$$

i.e. initial conditions with only adults present in the proportions of ν and $1-\nu$. This model separates the time scale of reproductive activity (daily) from the maturation period of juveniles, which is assumed here to be one season (or year).

To calculate the bifurcation value of ρ and to apply Theorem 1 we need to find a value of ρ such that $r(\rho, \hat{0}) = 1$ where $r(\rho, \hat{0})$ is given by (11), i.e. by

$$r(\rho, 0) = \hat{\nu}^{\tau} W^{k-1}(\rho, 0)\, \hat{a}$$

with matrix

$$W(\rho, 0) = \begin{pmatrix} 0 & 0 & b(\rho) & 0 \\ s_1 & s_2 & 0 & 0 \\ 0 & 0 & 0 & s_4 \\ 0 & 0 & s_3 & 0 \end{pmatrix}.$$

A simple calculation shows

$$W^2(\rho, 0) = \begin{pmatrix} 0 & 0 & 0 & b(\rho) s_4 \\ s_1 s_2 & s_2^2 & b(\rho) s_1 & 0 \\ 0 & 0 & s_3 s_4 & 0 \\ 0 & 0 & 0 & s_3 s_4 \end{pmatrix}$$

and an induction shows that the even and odd powers of $W(0)$ are, for $n = 2, 3, 4, ...,$

$$W^{2n}(\rho, 0) = \begin{pmatrix} 0 & 0 & 0 & b(\rho) s_4 (s_3 s_4)^{n-1} \\ s_1 s_2^{2n-1} & s_2^{2n} & b(\rho) A_{2n} & b(\rho) B_{2n} \\ 0 & 0 & (s_3 s_4)^n & 0 \\ 0 & 0 & 0 & (s_3 s_4)^n \end{pmatrix}$$

$$0 < A_{2n} := s_1 \sum_{i=1}^{n} (s_3 s_4)^{n-i} \left(s_2^2\right)^{i-1} = \begin{cases} s_1 \frac{(s_3 s_4)^n - \left(s_2^2\right)^n}{s_3 s_4 - s_2^2} & \text{if } s_3 s_4 \neq s_2^2 \\ n s_1 \left(s_2^2\right)^{n-1} & \text{if } s_3 s_4 = s_2^2 \end{cases}$$

$$0 < B_{2n} := s_1 s_2 s_4 \sum_{i=1}^{n-1} (s_3 s_4)^{n-1-i} \left(s_2^2\right)^{i-1} = \begin{cases} s_1 s_2 s_4 \frac{(s_3 s_4)^{n-1} - \left(s_2^2\right)^{n-1}}{s_3 s_4 - s_2^2} & \text{if } s_3 s_4 \neq s_2^2 \\ (n-1) s_1 s_2 s_4 \left(s_2^2\right)^{n-2} & \text{if } s_3 s_4 = s_2^2 \end{cases}$$

and

$$W^{2n-1}(\rho, 0) = \begin{pmatrix} 0 & 0 & b(\rho) (s_3 s_4)^{n-1} & 0 \\ s_1 s_2^{2n-2} & s_2^{2n-1} & b(\rho) A_{2n-1} & b(\rho) B_{2n-1} \\ 0 & 0 & 0 & s_4 (s_3 s_4)^{n-1} \\ 0 & 0 & s_3 (s_3 s_4)^{n-1} & 0 \end{pmatrix}$$

$$0 < A_{2n-1} := s_1 s_2 \sum_{i=1}^{n-1} (s_3 s_4)^{n-1-i} \left(s_2^2\right)^{i-1} = \begin{cases} s_1 s_2 \frac{(s_3 s_4)^{n-1} - \left(s_2^2\right)^{n-1}}{s_3 s_4 - s_2^2} & \text{if } s_3 s_4 \neq s_2^2 \\ s_1 s_2 (n-1) \left(s_2^2\right)^{n-2} & \text{if } s_3 s_4 = s_2^2 \end{cases}$$

$$0 < B_{2n-1} := s_1 s_4 \sum_{i=1}^{n-1} (s_3 s_4)^{n-1-i} \left(s_2^2\right)^{i-1} = \begin{cases} s_1 s_4 \frac{(s_3 s_4)^{n-1} - \left(s_2^2\right)^{n-1}}{s_3 s_4 - s_2^2} & \text{if } s_3 s_4 \neq s_2^2 \\ s_1 s_2 (n-1) \left(s_2^2\right)^{n-2} & \text{if } s_3 s_4 = s_2^2 \end{cases}$$

From these formulas we find that

$$r(\rho, 0) = \begin{cases} b(\rho) \left[\nu_1 (1-\nu) s_4 (s_3 s_4)^{n-1} + \nu_2 (\nu A_{2n} + (1-\nu) B_{2n})\right] & \text{if } k = 2n+1 \\ \quad + (\nu_3 \nu + \nu_4 (1-\nu)) (s_3 s_4)^n & \text{for } n = 1, 2, 3, ... \\ b(\rho) \left[\nu_1 \nu (s_3 s_4)^{n-1} + \nu_2 (\nu A_{2n-1} + (1-\nu) B_{2n-1})\right] & \text{if } k = 2n \\ \quad + [\nu_3 (1-\nu) s_4 + \nu_4 \nu s_3] (s_3 s_4)^{n-1} & \text{for } n = 2, 3, 4, ... \end{cases} \tag{21}$$

and that

$$r(0, 0) < 1, \quad \partial_\rho r(\rho, 0) > 0.$$

If $\lim_{\rho \to +\infty} r(\rho, 0) < 1$ then the extinction equilibrium is stable at all resource levels ρ. On the other hand, if

$$1 < \lim_{\rho \to +\infty} r(\rho, 0) \leq +\infty \tag{22}$$

then there exists a unique value of $\rho = \rho_0 > 0$ at which $r(\rho_0, 0) = 1$ and, therefore, for which Theorems 1 and 2 apply. In this case we conclude that *the two local bifurcation alternatives shown in the first row of plots in Figure 1 and the global bifurcation alternatives in Figure 2 apply to this model.*

Example correlations between adult fertility and environmental resource availability for which (22) holds are power laws

$$b(\rho) = b_0 \rho^q, \ b_0 > 0, \ q > 0$$

($\lim_{\rho \to +\infty} r(\rho, 0) = +\infty$) and saturating resource uptake rates

$$b(\rho) = b_0 \frac{\rho^q}{b_1 + \rho^q}, \ b_1 > 0, \ q > 0$$

provided, in that latter case, $b_0 = \lim_{\rho \to +\infty} b(\rho)$ is sufficiently large (so that (22) holds:

$$b_0 > \begin{cases} \frac{1 - (\nu_3 \nu + \nu_4 (1-\nu)) (s_3 s_4)^n}{\nu_1 (1-\nu) s_4 (s_3 s_4)^{n-1} + \nu_2 (\nu A_{2n} + (1-\nu) B_{2n})} & \text{if } k = 2n+1 \text{ for } n = 1, 2, 3, ... \\ \frac{1 - [\nu_3 (1-\nu) s_4 + \nu_4 \nu s_3] (s_3 s_4)^{n-1}}{\nu_1 \nu (s_3 s_4)^{n-1} + \nu_2 (\nu A_{2n-1} + (1-\nu) B_{2n-1})} & \text{if } k = 2n \text{ for } n = 2, 3, 4, ... \end{cases}.$$

We are particularly interested circumstances when a backward bifurcation occurs since, as discussed in Section 2.2, this leads to (initial condition dependent) survival in severely degraded environments, i.e. when $r(\rho, 0) < 1$ and the extinct equilibrium is stable. Corollary 1 tells us that a backward bifurcation occurs when there are dominant positive effects of low density increases (component Allee effects), i.e. positive state variable derivatives of the entries (18) of the projection matrix W (evaluated at $\hat{x} = \hat{0}$).

There are both negative and positive density effects in the entries (18) of W. Specifically, negative low density effects occur in w_{12} from the assumed adult x_3 and x_4 density regulation of

fertility ($\varphi'(z) < 0$) and in w_{21} with respect to x_3 and x_4 from the effect of cannibalism on egg survival ($\partial_{x_i}\pi_i \geq 0$). Positive low density effects occur w_{34}, w_{43}, w_{44} with respect to x_3 and x_4 from the assumed positive effect of cannibalism on adult survival ($\sigma_i'(z) > 0$).

Finally, the adult reproductive synchrony term $g(x_3)$ contributes a negative feedback to w_{34}, but a positive feedback to w_{44} ($g' < 0$). Therefore, the net contribution of g to a backward bifurcation is equivocal and, as we will see from Examples 1 and 2, depends on model's inherent parameter values, namely the survivorships s_i and ν_i and the season length $k-1$.

By Theorem 1 one can, determine the direction of bifurcation from the sign of $\partial_\alpha^0 r$ which, in principle, can be calculated from the formula

$$\partial_\alpha^0 r = \partial_\alpha \hat{\nu}^\tau Q(p,\alpha)\,\hat{a}|_{(p,\alpha)=(p_0,0)}\,.$$

The formula is, however, sufficiently complicated that little in the way of general conclusions can be discerned from it beyond those in Corollary 1; see the Appendix. Nonetheless, we can conclude from Corollary 1 that *if the benefit to adult survival from cannibalism is sufficient high, then a backward bifurcation will occur. The general effect of reproductive synchrony, i.e. of the g, on the direction of bifurcation, however, remains ambiguous and model parameter dependent.* See Examples 1 and 2.

We illustrate these conclusions will some selected simulations. We use the nonlinearities

$$\varphi(z) = \frac{1}{1 + c_{\varphi 3}x_3 + c_{\varphi 4}x_4}, \quad b(\rho) = b_0\rho \tag{23a}$$

$$\pi_j(x_1, x_j) = \frac{1}{1 + w_1 x_1}\frac{\omega_j(\rho)}{1 + \omega_j(\rho)\,x_j}, \quad \omega_j(\rho) = \frac{w_j}{1 + c_\rho \rho} \tag{23b}$$

$$\sigma_j(x_1, x_j) = 1 + \frac{s_{jm} - s_j}{s_j}\frac{c_{\sigma j} z}{1 + c_{\sigma j} z}, \quad g(x_3) = \frac{1}{1 + c_g x_3} \tag{23c}$$

All of the coefficients associated with these nonlinearities are nonnegative. By setting a coefficient equal to zero, the corresponding linear mechanism is removed from the model. For example, $c_{\sigma j} = 0$ removes the positive benefit of cannibalism to the survival probability of adult x_j, $c_g = 0$ removes the synchrony propensity, $w_j = 0$ removes cannibalism by x_j, and $w_1 = 0$ removes the victim saturation effect, etc. It is assumed that $0 < s_j < s_{jm} < 1$ so that the survival component $s_j\sigma_j$ increases from s_j to s_{jm} as the number of cannibalized eggs z increases from 0 to $+\infty$. Increasing the value of a coefficient, increases the effect (or intensity) of the corresponding nonlinear mechanism.

These nonlinearities satisfy all of the requirements laid out above and, in particular, satisfy (22). Using the environmental resource availability $p = \rho$ as a bifurcation parameter, we calculate the unique bifurcation value

$$\rho_0 = \begin{cases} \frac{1}{b_0}\frac{1-(\nu_3\nu+\nu_4(1-\nu))(s_3s_4)^n}{\nu_1(1-\nu)s_4(s_3s_4)^{n-1}+\nu_2(\nu A_{2n}+(1-\nu)B_{2n})} & \text{if } k = 2n+1 \text{ for } n = 1,2,3,... \\ \frac{1}{b_0}\frac{1-[\nu_3(1-\nu)s_4+\nu_4\nu s_3](s_3s_4)^{n-1}}{\nu_1\nu(s_3s_4)^{n-1}+\nu_2(\nu A_{2n-1}+(1-\nu)B_{2n-1})} & \text{if } k = 2n \text{ for } n = 2,3,4,... \end{cases}.$$

from (21) at which, according to Theorems 1 and 2, the forward and backward bifurcation alternatives shown in Figure 2 hold.

Example 1 *For the parameter values displayed in the caption, Figure 4 shows two bifurcation diagrams that plot the total population size α of the attractor at the beginning of the season as a function of the environmental resource availability ρ. Cannibalism is in effect and the bifurcations are backward, creating a strong Allee effect in a severely degraded environment. By this we mean (initial*

condition dependent) survival for an interval of environmental resource levels ρ below ρ_0 where the inherent population growth rates $r(0)$ are less than 1. The bifurcation diagram with $c_g = 0$ (when the synchrony propensity term is absent) illustrates a cannibalism induced backward bifurcation. (If cannibalism were also absent, then the bifurcation would be forward since there would then be no positive density effects; see Corollary 1.) In this sense, cannibalism in this example is beneficial since it allows for non-extinction in an adverse environment when the absence of cannibalism would result in extinction.

The bifurcation diagram with $c_g > 0$ indicates added benefits toward the survival of the population due to reproductive synchrony in two senses: the presence of the synchrony propensity term results in a higher total population size (at the start of each season), at any environmental resource level ρ, and also a reduced environmental resource "tipping" point" where the saddle node bifurcation leads to catastrophic-extinction.

Figure 5 shows some sample time series at the indicated locations on the bifurcation diagrams. Note the within season adult class synchronized oscillations when $c_g > 0$ and their absence when $c_g = 0$.

Example 2 *The sample simulations in Example 1 show a benefit of reproductive synchrony in a cannibalistic population. This is not, however, always predicted by the model. The two bifurcation diagrams in Figure 6 show the opposite, namely, that reproductive synchrony reduces population size and increases the tipping point for the environmental resource availability. These diagrams use the same within-season parameter values as in Figure 5, but change the across season survival probabilities as indicated in the captions.*

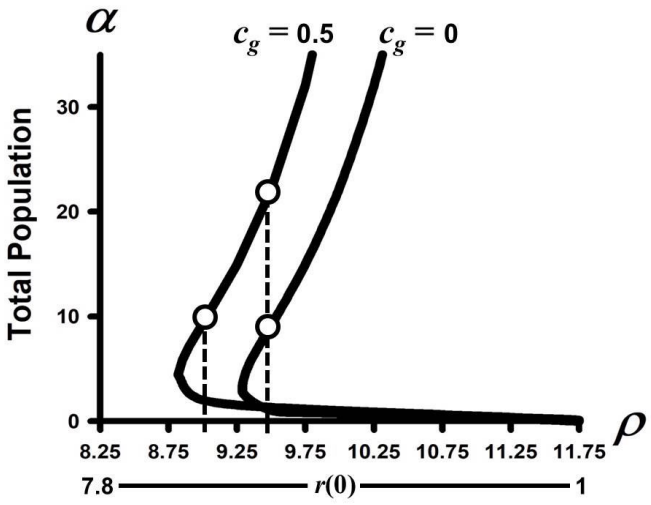

Figure 4. Shown are two backward bifurcation diagrams plotting total population size a at the beginning of the season of the attractor as a function of the environmental resource availability ρ using the nonlinearities (23) in (15) with projection matrices (17) and (19). In one plot ($c_g = 0$), the synchrony propensity term is absent and in the other plot ($c_g = 0.5$) it is present. Parameter values are $b_0 = 0.7$, $c_{\varphi 3} = c_{\varphi 4} = 0.001$, $c_\rho = 1$, $c_{\sigma 3} = c_{\sigma 4} = 1$, $w_1 = 1$, $w_3 = w_4 = 2$, $s_1 = s_2 = 0.3$, $s_3 = s_4 = 0.9$, $s_{3m} = s_{4m} = 0.99$

and $\nu_1 = \nu_2 = \nu_4 = \nu_5 = 0.95$. The bifurcation value is $\rho_0 \approx 11.75$. Sample time series plots at the open circles are shown in Figure 5.

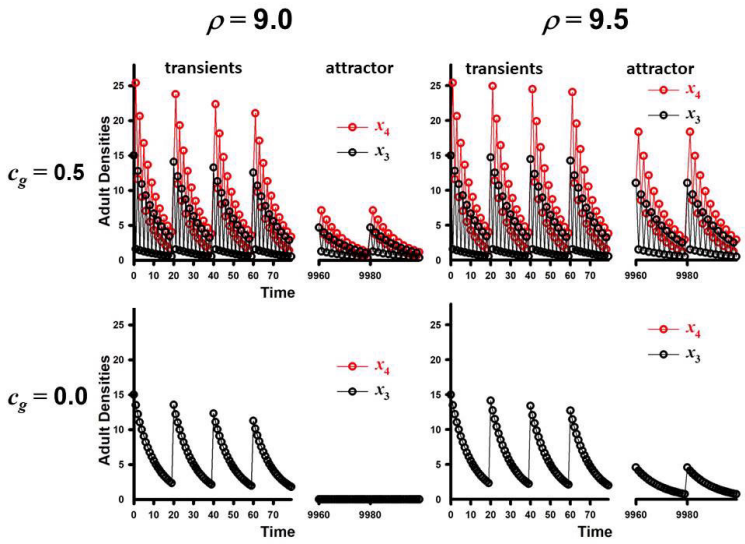

Figure 5. Sample adult class time series are shown for initial conditions $x_1 = x_2 = 0$, $x_3 = \nu\alpha$, $x_4 = \alpha(1-\nu)$ with $\nu = 0.5$ and $\alpha = 30$. The first column of plots are for $\rho = 9.0$ and the second column of are for $\rho = 9.5$ (cf. to the open circles shown in Figure 4).

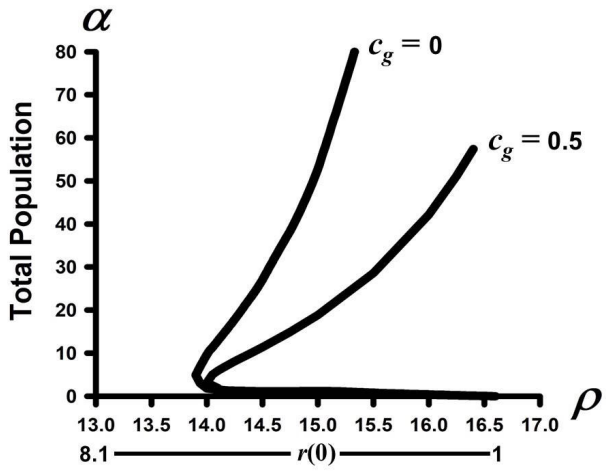

Figure 6. Shown are the same two bifurcation plots that appear in Figure 4, with the same parameter values except for a change in the across season survival probabilities to $\nu_1 = 0.5$, $v_2 = \nu_3 = \nu_4 = 0.99$. .

4 Concluding remarks

Average SSTs have been rising in the Salish Sea and are expected to continue to rise. High SSTs are associated with low food resources for surface-feeding marine birds such as glaucous-winged gulls, and such seabirds are considered sentinels of environmental change. At the Protection Island colony, high SSTs are associated with behavioral changes including high egg cannibalism and the onset of daily egg-laying synchrony. How do such behavioral changes on a daily time scale within the breeding season affect population dynamics across seasons? What consequences do they have for the long term survival of the populations?

Motivated by these questions for seabirds, we formulate in Section 2 a general class of periodically-forced structured matrix models that describes the behavioral and reproductive dynamics within each breeding season and then projects the population to the next breeding season. Since the question of extinction-versus-survival is of primary concern, especially in view of climate change, we focus on the extinction equilibrium and its destabilization in our analysis of these models. We show that a study of the seasonal composite map, which maps the demographic vector at the beginning of one season to the beginning of the next season, reduces to the study of a scalar map from which the theorems of Section 2 are derived. The general results in Section 2.1 account for the bifurcation of non-extinction seasonal cycles at a critical value of model parameters at which the extinction equilibrium destabilizes, the direction of bifurcation of these cycles and their stability near the bifurcation point. Stability depends on the direction of bifurcation (an example of the exchange of stability principle for transcritical bifurcations). Section 2.2 takes advantage of the reduction to a scalar map to give results on the global extent of the bifurcating cycles and their stability outside a neighborhood of the bifurcation point.

In Section 3 we consider a specific example from this general class of models as applied to the seabird system. We focus on egg cannibalism and the daily reproductive synchrony of female egg laying. The mechanisms built into the model include: the negative and positive effects of egg cannibalism on juveniles and on adult survival; the positive effect of cannibal (predator) saturation effect by victim (prey) density; and the negative effect of adult density regulation of fertility. The model separates two time scales, the within-(breeding) season time scale when egg laying synchrony takes place and the across-season time scale at which juvenile maturation occurs. This time scale separation is absent in previous models investigating cannibalism and reproductive synchrony [9], [32], with the exception of the model in [14], of which our model here is significant extension.

Of particular interest in the bifurcation scenarios derived in Section 2 is the case of a backward, and hence unstable, bifurcation of non-extinction seasonal cycles. As shown in Section 2.2, backward bifurcations typically produce strong Allee effects in population models. A strong Allee effect is, by definition, a multiple attractor scenario containing both a non-extinction attractor and a stable extinction equilibrium. In this scenario, initial condition dependent survival is possible prior to the destabilization of the extinction equilibrium, corresponding presumably to poor or degraded environmental conditions. In this sense, a *backward bifurcation is beneficial* to the population. The diagnostic quantity ($\partial_\alpha^0 r$) that determines the direction of bifurcation is shows that positive density effects at low densities (component Allee effects) must be present and of sufficient significance in order for a backward bifurcation to occur. The gull model in Section 3 has both positive and negative effects and can exhibit backward or forward bifurcations, depending on parameter values. It is shown in that section, and its examples, that the positive effects of the reproductive synchrony propensity and of cannibalism on adult survival can lead to a backward bifurcation and therefore can produce the survival benefits of a backward bifurcation. It is also seen from Examples 1

and 2 how under some circumstances (i.e. some inherent within-season and across-season survival values, season lengths and cannibalism intensities) the benefit of a higher total population size can also accrue from reproductive synchrony, although under other circumstances a lower total populations size might occur. Thus, we see in this model how certain individual behaviors affect the population-level dynamics and how benefits to individuals might or might not be a benefit to the total population.

Although the gull-inspired model in Section 3 is more realistic than our previous proof-of-concept models, two major simplifications still separate it from the motivating system. First, the model assumes that each surviving adult female can continue to lay eggs throughout the breeding season, whereas in reality each female lays approximately three eggs during the season. Second, the model assumes that all surviving juveniles become adults at the beginning of the next breeding season, whereas juvenile glaucous-winged gulls actually require four years to mature. There are a number of smaller simplifications, as well. For example, the model does not keep track of egg order in a nest, and so any egg (not just the first egg in the nest) can be cannibalized on the day it is laid, whereas in glaucous-winged gulls the first egg is the most likely of the eggs in a clutch to be cannibalized. The general class of models can be extended to meet these requirements. Another class of individuals (incubating females) could be followed, and the maturation period of juveniles could be lengthened to more than one season. This would involve creating yet a larger demographic vector to include juveniles of differing ages, only the oldest of which matures from one season to the next. The result would be a higher dimensional matrix model, with higher dimensional within-season and across-season matrices W and A. Although there would be a dimensional reduction for the dynamics of the composite map from start of season to start of season, it would no longer necessarily be a reduction to dimension one. The resulting periodically-forced model would therefore be more demanding to analyze. Another enhancement of the model would include density effects on across-season survival ($\nu_i = \nu_i(\hat{x})$), which were ignored here. In this case the dynamics of the resulting periodically-forced models in Section 2 would still be reducible to a scalar map, but with additional nonlinearities that need to be modeled, and the Theorems in Section 3 would still hold.

In conclusion, changes in individual behavioral tactics on a daily time scale within a breeding season in response to environmental change can affect population-level dynamics across seasons. Behaviors such as egg cannibalism and egg-laying synchrony that afford an adaptive advantage to individuals may lead to population-level Allee effects that allow populations to survive at lower resources levels than they would otherwise. These strong Allee effects, however, are associated with initial-condition-dependent survival thresholds and with tipping points at resource levels below which the population suffers collapse.

Acknowledgements We thank James L. Hayward for field work collaboration and discussions; Jennifer Brown-Scott, Lorenz Sollmann, and Sue Thomas, Washington Maritime National Wildlife Refuge Complex, for permission to work on Protection Island National Wildlife Refuge; and Rosario Beach Marine Laboratory for logistical support. We thank two anonymous reviewers for their careful reading of the manuscript and their suggestions for its revision. This research was supported by the U. S. National Science Foundation grants DMS-1407564 (JMC) and DMS-1407040 (SMH).

Appendix

The following Lemma is an extension of results in [8]).

Lemma 1 *Assume A1 and A2.*

(a) Suppose $\partial_p^0 r > 0$. Then the equilibrium $\alpha = 0$ of the difference equation (12) is locally asymptotically stable if $p < p_0$ and is unstable if $p > p_0$. Suppose, on the other hand, that $\partial_p^0 r < 0$. Then $\alpha = 0$ is locally asymptotically stable for $p > p_0$ and is unstable for $p < p_0$.

(b) On an open interval I of p_0 there exists a (twice continuously differentiable) continuum of equilibria $\alpha = \alpha(p)$ of the difference equation (12) satisfying $\alpha(p_0) = 0$ and $\alpha(p) \neq 0$ for $p \neq p_0$.

(c) Suppose $\partial_p^0 r > 0$. If $\partial_\alpha^0 r < 0$ then for $p \in I$ the equilibrium $\alpha(p)$ is positive and locally asymptotically stable if $p > p_0$ (and are negative for $p < p_0$). On the other hand, if $\partial_\alpha^0 r > 0$ then for $p \in I$ the equilibrium $\alpha(p)$ is positive and unstable for $p < p_0$ (and are negative for $p > p_0$).

(d) Suppose $\partial_p^0 r < 0$. If $\partial_\alpha^0 r > 0$ then for $p \in I$ the equilibrium $\alpha(p)$ is positive and locally asymptotically stable for $p > p_0$ (and are negative for $p < p_0$). On the other hand, if $\partial_\alpha^0 r < 0$ then for $p \in I$ the equilibrium $\alpha(p)$ is positive and unstable for $p > p_0$ (and are negative for $p > p_0$).

Proof. (a) The linearization principle guarantees local asymptotic stability of $\alpha = 0$ if $r(0,p) < 1$ and instability if $r(0,p) > 1$.

(b) Under assumption A2 we can apply the implicit function theorem to the equation $r(p,\alpha) = 1$ for nontrivial equilibria of the difference equation (12) and obtain, on an open interval of p_0, a twice continuously differentiable function $\alpha = \alpha(0)$, $\alpha(p_0) = 0$ satisfying $r(p, \alpha(p)) = 1$. An implicit differentiation with respect to p yields $\alpha'(0) = -\partial_p^0 r / \partial_\alpha^0 r \neq 0$ from which it follows that $\alpha(p) \neq 0$ for $p \neq p_0$.

(c) If $\alpha'(0) > 0$ then $\alpha(p) > 0$ (respectively $\alpha(p) < 0$) for $p \gtrapprox p_0$ (respectively $p \lessapprox p_0$. On the other hand, if $\alpha'(0) < 0$ then $\alpha(p) > 0$ (respectively $\alpha(p) < 0$) for $p \lessapprox p_0$ (respectively $p \gtrapprox p_0$) as asserted. With regard to the stability of the equilibrium $\alpha(p)$ for p near p_0, we apply the linearization principle by calculating

$$\begin{aligned} \left.\frac{\partial(r(p,\alpha)\alpha)}{\partial\alpha}\right|_{\alpha=\alpha(p)} &= 1 + \alpha(p) \left.\frac{\partial(r(p,\alpha))}{\partial\alpha}\right|_{\alpha=\alpha(p)} \\ &= 1 + \left(\alpha'(0)\,\partial_\alpha^0 r\right)(p - p_0) + O\left((p-p_0)^2\right) \\ &= 1 + \left(-\partial_p^0 r\right)(p - p_0) + O\left((p-p_0)^2\right). \end{aligned} \tag{24}$$

Assume $\partial_p^0 r > 0$. If $\partial_\alpha^0 r < 0$ then $\alpha'(0) = -\partial_p^0 r / \partial_\alpha^0 r > 0$ and $\alpha(p)$ is positive and $|\lambda| < 1$ for $p \gtrapprox p_0$. If $\partial_\alpha^0 r > 0$ then $\alpha'(0) = -\partial_p^0 r / \partial_\alpha^0 r < 0$ and $\alpha(p)$ is positive and $|\lambda| < 1$ for $p \lessapprox p_0$.

(d) These conclusions are derived in closely similar manner to those in (c) by also making use of (24).

Proof of Corollary 1. It is obvious from the definition of $\hat{x}(t,\alpha)$ that $\hat{x}(t,0) = \hat{0}$ for all t. From (10) we have

$$\partial_\alpha^0 r = \hat{\nu} \partial_\alpha^0 Q \hat{a}$$

where

$$Q(\alpha) = \prod_{k-2}^{t=0} W(\hat{x}(t)) = W(\hat{x}(k-2)) \cdots W(\hat{x}(1)) W(\hat{x}(0))$$

$$\partial_\alpha^0 Q = \frac{\partial}{\partial \alpha} \prod_{k-2}^{t=0} W\left(\hat{x}\left(t\right)\right)\Big|_{\alpha=0} = \sum_{t=0}^{k-2} W^{k-2-t}(\hat{0})\ \frac{\partial}{\partial \alpha} W\left(\hat{x}\left(t\right)\right)\Big|_{\alpha=0} W^t(\hat{0})$$

By the chain rule

$$\frac{\partial}{\partial \alpha} W\left(\hat{x}\left(t\right)\right)\Big|_{\alpha=0} = \left[\nabla_{\hat{x}}^0 w_{ij}\ \frac{\partial}{\partial \alpha}\hat{x}\left(t\right)\Big|_{\alpha=0}\right]$$

where

$$\nabla_{\hat{x}}^0 w_{ij} = \left(\ \partial_{x_1}^0 w_{ij} \quad \partial_{x_2}^0 w_{ij} \quad \cdots \quad \partial_{x_m}^0 w_{ij}\ \right).$$

From

$$\hat{x}\left(t\right) = \left(\prod_{t-1}^{i=0} W\left(\hat{x}\left(i\right)\right)\right)\alpha\hat{a}$$

we obtain

$$\frac{\partial}{\partial \alpha}\hat{x}\left(t\right)\Big|_{\alpha=0} = W^t\left(0\right)\hat{a}$$

for $t = 0, 1, \cdots, k-1$. The matrix

$$D\left(t\right) := \frac{\partial}{\partial \alpha} W\left(\hat{x}\left(t\right)\right)\Big|_{\alpha=0} = \left[\nabla_{\hat{x}}^0 w_{ij} W^t\left(0\right)\hat{a}\right]$$

leads to

$$\partial_\alpha^0 Q = \sum_{t=0}^{k-2} W^{k-2-t}(\hat{0}) D\left(t\right) W^t(\hat{0}).$$

The entries in the matrix $D\left(t\right)$ are linear combinations of the derivatives $\partial_{x_l}^0 w_{ij}$. It follows that the same is true of the entries in the matrix $\partial_\alpha^0 Q$ and, as a result, the same is true of $\partial_\alpha^0 r$.

The quantity $\partial_\alpha^0 r$ for the gull model (17)–(19) with (18) We use the formula

$$\partial_\alpha^0 r = \hat{\nu}^\tau \partial_\alpha Q\left(p, \alpha\right)\hat{a}|_{(p,\alpha)=(p_0,0)}$$

where

$$\partial_\alpha Q\left(p, \alpha\right) = \partial_\alpha \prod_{k-2}^{t=0} W\left(p, \hat{x}\left(t\right)\right)$$

with matrix W defined by (17) and entries (18) and with the vectors $\hat{\nu}^\tau$ and $\hat{a}$ given by (20). By the product rule

$$\partial_\alpha^0 Q = \sum_{t=0}^{k-2} W^{k-2-t}(\hat{0}) D\left(t\right) W^t(\hat{0})$$

where

$$D\left(t\right) := \left[\nabla_{\hat{x}}^0 w_{ij}\ \frac{d\hat{x}\left(i\right)}{d\alpha}\Big|_{\alpha=0}\right] = \left[\nabla_{\hat{x}}^0 w_{ij} W^t\left(0\right)\hat{a}\right]$$

since

$$\hat{x}\left(i\right) = \left(\prod_{t=0}^{i-1} W\left(\hat{x}\left(t\right)\right)\right)\alpha\hat{a}$$

implies

$$\left.\frac{d\hat{x}\left(i\right)}{d\alpha}\right|_{\alpha=0}=W^{i}(\hat{0})\hat{a}.$$

From the gull model matrix entries (18) we have

$$D\left(t\right)=\left(\begin{array}{cccc}
0 & 0 & p_{0}\nabla_{\hat{x}}^{0}\varphi W^{t}\left(0\right)\hat{a} & 0\\
-s_{1}\nabla_{\hat{x}}^{0}\left(\pi_{3}\left(x_{1},x_{3}\right)x_{3}\right)W^{t}\left(0\right)\hat{a} & 0 & 0 & 0\\
-s_{1}\nabla_{\hat{x}}^{0}\left(\pi_{4}\left(x_{1},x_{4}\right)x_{4}\right)W^{t}\left(0\right)\hat{a} & & & \\
0 & 0 & 0 & s_{4}\nabla_{\hat{x}}^{0}\left(\beta_{4}g\right)W^{t}\left(0\right)\hat{a}\\
0 & 0 & s_{3}\nabla_{\hat{x}}^{0}\beta_{3}W^{t}\left(0\right)\hat{a} & s_{4}\nabla_{\hat{x}}^{0}\left(\beta_{4}\left(1-g\right)\right)W^{t}\left(0\right)\hat{a}
\end{array}\right)$$

Let M_{ij} be the 4×4 matrices with all zero entries with the exception of a 1 in the ij^{th} entry. Making use of these matrices, we write

$$\begin{aligned}
D\left(t\right)=&-s_{1}\left(\begin{array}{cccc}0 & 0 & \pi_{3}\left(0,0\right) & \pi_{4}\left(0,0\right)\end{array}\right)W^{t}\left(0\right)\hat{a}M_{21}+p_{0}\nabla_{\hat{x}}^{0}\varphi W^{t}\left(0\right)\hat{a}M_{13}\\
&+s_{3}\nabla_{\hat{x}}^{0}\beta_{3}W^{t}\left(0\right)\hat{a}M_{43}+s_{4}\nabla_{\hat{x}}^{0}\left(\beta_{4}g\right)W^{t}\left(0\right)\hat{a}M_{34}\\
&+s_{4}\nabla_{\hat{x}}^{0}\left(\beta_{4}\left(1-g\right)\right)W^{t}\left(0\right)\hat{a}M_{44}.
\end{aligned}$$

Then

$$\begin{aligned}
\hat{\nu}^{\tau}W^{k-2-t}(\hat{0})D\left(t\right)W^{t}(\hat{0})\hat{a}=&-s_{1}c_{0}\left(t\right)\left(\begin{array}{cccc}0 & 0 & \pi_{3}\left(0,0\right) & \pi_{4}\left(0,0\right)\end{array}\right)W^{t}\left(0\right)\hat{a}\\
&+p_{0}c_{1}\left(t\right)\nabla_{\hat{x}}^{0}\varphi W^{t}\left(0\right)\hat{a}\\
&+s_{3}c_{2}\left(t\right)\nabla_{\hat{x}}^{0}\beta_{3}W^{t}\left(0\right)\hat{a}+s_{4}c_{3}\left(t\right)\nabla_{\hat{x}}^{0}\left(\beta_{4}g\right)W^{t}\left(0\right)\hat{a}\\
&+s_{4}c_{4}\left(t\right)\nabla_{\hat{x}}^{0}\left(\beta_{4}\left(1-g\right)\right)W^{t}\left(0\right)\hat{a}
\end{aligned}$$

where we defined the nonnegative scalar coefficients

$$\begin{aligned}
&c_{0}\left(t\right):=\hat{\nu}^{\tau}W^{k-2-t}(\hat{0})M_{21}W^{t}(\hat{0})\hat{a},\quad c_{1}\left(t\right)=\hat{\nu}^{\tau}W^{k-2-t}(\hat{0})M_{13}W^{t}(\hat{0})\hat{a}\\
&c_{2}\left(t\right)=\hat{\nu}^{\tau}W^{k-2-t}(\hat{0})M_{43}W^{t}(\hat{0})\hat{a},\quad c_{3}\left(t\right)=\hat{\nu}^{\tau}W^{k-2-t}(\hat{0})M_{34}W^{t}(\hat{0})\hat{a}\\
&c_{4}\left(t\right)=\hat{\nu}^{\tau}W^{k-2-t}(\hat{0})M_{44}W^{t}(\hat{0})\hat{a}.
\end{aligned}$$

This leads to

$$\begin{aligned}
\partial_{\alpha}^{0}r=&\sum_{t=0}^{k-2}\hat{\nu}^{\tau}W^{k-2-t}(\hat{0})D\left(t\right)W^{t}(\hat{0})\hat{a}\\
=&-s_{1}\sum_{t=0}^{k-2}c_{0}\left(t\right)\left(\begin{array}{cccc}0 & 0 & \pi_{3}\left(p_{0},0,0\right) & \pi_{4}\left(p_{0},0,0\right)\end{array}\right)W^{t}\left(0\right)\hat{a}+p_{0}\sum_{t=0}^{k-2}c_{1}\left(t\right)\left[\nabla_{\hat{x}}^{0}\varphi W^{t}\left(0\right)\hat{a}\right]\\
&+s_{3}\sum_{t=0}^{k-2}c_{2}\left(t\right)\left[\nabla_{\hat{x}}^{0}\beta_{3}W^{t}\left(0\right)\hat{a}\right]+s_{4}\sum_{t=0}^{k-2}c_{3}\left(t\right)\left[\nabla_{\hat{x}}^{0}\beta_{4}W^{t}\left(0\right)\hat{a}\right]\\
&+s_{4}\sum_{t=0}^{k-2}\left(c_{3}\left(t\right)-c_{4}\left(t\right)\right)\left[\nabla_{\hat{x}}^{0}gW^{t}\left(0\right)\hat{a}\right].
\end{aligned}$$

Finally, making use of

$$\nabla_{\hat{x}}\left(\beta_4 g\right) = g\nabla_{\hat{x}}\beta_4 + \beta_4\nabla_{\hat{x}}g \Rightarrow \nabla^0_{\hat{x}}\left(\beta_4 g\right) = \nabla^0_{\hat{x}}\beta_4 + \nabla^0_{\hat{x}}g$$

$$\nabla_{\hat{x}}\left(\beta_4\left(1-g\right)\right) = \left(1-g\right)\nabla_{\hat{x}}\beta_4 - \beta_4\nabla_{\hat{x}}g \Rightarrow \nabla^0_{\hat{x}}\left(\beta_4\left(1-g\right)\right) = -\nabla^0_{\hat{x}}g$$

we arrive at

$$\begin{aligned}
\partial^0_\alpha r = &-s_1\sum_{t=0}^{k-2} c_0\left(t\right)\begin{pmatrix} 0 & 0 & \pi_3\left(p_0,0,0\right) & \pi_4\left(p_0,0,0\right)\end{pmatrix} W^t\left(0\right)\hat{a}\\
&+\varphi'\left(0\right)p_0\sum_{t=0}^{k-2} c_1\left(t\right)\begin{pmatrix} 0 & 0 & c_{\varphi 3} & c_{j4}\end{pmatrix} W^t\left(0\right)\hat{a}\\
&+\sigma_3'\left(0\right)s_3\sum_{t=0}^{k-2} c_2\left(t\right)\begin{pmatrix} \pi_3\left(p_0,0,0\right) & 0 & 0 & 0\end{pmatrix} W^t\left(0\right)\hat{a}\\
&+\sigma_4'\left(0\right)s_4\sum_{t=0}^{k-2} c_3\left(t\right)\begin{pmatrix} \pi_4\left(p_0,0,0\right) & 0 & 0 & 0\end{pmatrix} W^t\left(0\right)\hat{a}\\
&+g'\left(0\right)s_4\sum_{t=0}^{k-2}\left(c_3\left(t\right)-c_4\left(t\right)\right)\begin{pmatrix} 0 & 0 & 1 & 0\end{pmatrix} W^t\left(0\right)\hat{a}.
\end{aligned}$$

The first two terms, deriving from the adult density dependent fertility and the effect of cannibalism on egg survival, are negative and therefore contribute to a forward bifurcation. The third and fourth terms are positive, deriving from the positive density effect of cannibalism on adult survival. Finally the sign of the last term, which involves the synchrony term $g'\left(0\right) < 0$, is ambiguous due to the difference $c_3\left(t\right) - c_4\left(t\right)$ whose sign is dependent on model parameters.

References

[1] Alvarez-Fernandez S, Licandro P, van Damme CJG, Hufnagl M (2015) Effect of zooplankton on fish larval abundance and distribution: A long-term study on North Sea herring (*Clupea harengus*), ICES Journal of Marine Science 72, Issue 9:2569-2577

[2] Barber RT, Chavez FP (1983) Biological consequences of El Niño, Science 222:1203-1210

[3] Blight LK (2011) Egg production in a coastal seabird, the Glaucous-winged Gull (*Larus glaucescens*), declines during the last century. PLoS ONE 6, Issue 7:1-8

[4] Burton D, Henson SM (2014) A note on the onset of synchrony in avian ovulation cycles, Journal of Difference Equations and Applications 20:664–668

[5] Caswell H, Trevisan MC (1994) Sensitivity analysis of periodic matrix models. Ecology 75:1299-303

[6] Caswell H (2001) Matrix population models: construction, analysis, and interpretation. Second edition. Sinauer Associates, Sunderland, Massachusetts, USA

[7] Cushing JM (2014) Backward bifurcations and strong Allee effects in matrix models for the dynamics of structured populations, Journal of Biological Dynamics 8: 57-73

[8] Cushing JM (2016) One dimensional maps as population and evolutionary dynamic models, Applied Analysis in Biological and Physical Sciences, Springer Proceedings in Mathematics & Statistics, Volume 186, (JM Cushing, M Saleem, HM Srivastava, MA Khan, M Merajuddin, eds.), Springer, India, pp. 41-62

[9] Cushing JM, Henson SM, Hayward JL (2015) An evolutionary game theoretic model of cannibalism, Natural Resource Modeling 28, No. 4: 497-52

[10] Galusha JG, Vorvick B, Opp M, Vorvick P (1987) Nesting season censuses of seabirds on Protection Island, Washington. The Murrelet 68:103–107

[11] Hayward JL, Verbeek NA (2008) Glaucous-winged gull (*Larus glaucescens*), The Birds of North America Online, A. Poole, ed., Cornell Laboratory of Ornithology, Ithaca, NY. Available from The Birds of North America at http://bna.birds.cornell.edu/bna/species/059

[12] Hayward JL, Weldon LM, Henson SM, Megna LC, Payne BG, Moncrieff AE (2014) Egg cannibalism in a gull colony increases with sea surface temperature The Condor: Ornithological Applications 116:62–73

[13] Henson SM, Hayward JL, Cushing JM, Galusha JG (2010) Socially induced synchronization of every-other-day egg laying in a seabird colony, Auk 127:571–580

[14] Henson SM, Cushing JM, Hayward JL (2011) Socially-induced ovulation synchrony and its effect on seabird population dynamics, Journal of Biological Dynamics 5:495-516

[15] Henson SM, Hayward JL, personal communication

[16] Irvine JR, Crawford WR (2011) State of the Ocean Report for the Pacific North Coast Integrated Management Area (PNCIMA). Nanaimo, BC: Fisheries and Oceans Canada, Science Branch, Pacific Region, Pacific Biological Stations

[17] Irvine JR, Crawford WR (2013) State of Physical, Biological, and Selected Fishery Resources of Pacific Canadian Marine Ecosystems in 2012. Research Document 2013/032. Ottawa, ON: Canadian Science Advisory Secretariat, Fisheries and Oceans Canada, Pacific Region

[18] Kershner J, Samhouri JF, James CA, Levin PS (2011) Selecting indicator portfolios for marine species and food webs: a Puget Sound case study. PLoS ONE 6:e25248

[19] Kielhöfer H (2004) Bifurcation Theory: An Introduction with Applications to PDEs, Applied Mathematical Sciences 156, Springer, New York

[20] Lesnoff M (1999) Dynamics of a sheep population in a Sahelian area (Ndiagne district in Senegal): a periodic matrix model, Agricultural Systems 61:207-221

[21] Lesnoff M, Lancelot R. Tillard E, Dohoo IR (2000) A steady-state approach of benefit-cost analysis with a periodic Leslie-matrix model: presentation and application to the evaluation of a sheep-diseases preventive scheme in Kolda, Senegal, Preventive Veterinary Medicine 46:113-128

[22] McGowan JA, Cayan DR, Dorman LM (1998) Climate ocean variability and ecosystem response in the northeast Pacific, Science 281:210-217

[23] Mertens SK, Yearsley JM, van den Bosch F, Gilligan CA (2006) Transient population dynamics in periodic matrix models: methodology and effects of cyclic permutations, Ecology 87(9):2338-2348

[24] Pearson SF, Hodum PJ, Good TP, Schrimpf M, Knapp SM (2013) A model approach for estimating colony size, trends, and habitat associations of burrow-nesting seabirds. Condor 115:356-365

[25] Sandberg S, Awerbuch TE, Spielman A (1992) A Comprehensive Multiple Matrix Model Representing the Life Cycle of the Tick that Transmits the Agent of Lyme Disease, Journal of Theoretical Biology 157:203-220

[26] Sarukhan J, Gadgil M (1974) Studies on plant demography: *Ranunculus repens* L., *R. bulbosus* L. and *R. acris* L. Ill. A mathematical model incorporating multiple modes of reproduction. Journal of Ecology 62:921-936

[27] Schreiber S (2003), Allee effects, extinctions, and chaotic transients in simple population models,Theoretical Population Biology 64:201-209

[28] Schreiber RW, Schreiber EA (1984) Central Pacific seabirds and the El Niño Southern Oscillation: 1982 to 1983 perspectives, Science 225:713-716

[29] Smith RS, Weldon LM, Hayward JL, Henson SM (2017) Time lags associated with effects of oceanic conditions on seabird breeding in the Salish Sea region of the northern California Current system, Marine Ornithology 45:39-42.

[30] Stenseth NC, Mysterud A, Ottersen G, Hurrell JW, Chan K-S, Lima M (2002) Ecological effects of climate fluctuations. Science 297:1292-1296

[31] Strom A, Francis RC, Mantua NJ, Miles EL, Peterson DL (2004) North Pacific climate recorded in growth rings of geoduck clams: a new tool for paleoenvironmental reconstruction, Geophysical Research Letters 31, Issue 6, DOI: 10.1029/2004GL019440

[32] Veprauskas A, Cushing JM (2017) A juvenile-adult population model: climate change, cannibalism, reproductive synchrony, and strong Allee effects, Journal of Biological Dynamics 11:1-24

[33] Vermeer K (1963) The breeding ecology of the glaucous-winged gull (*Larus glaucescens*), Occasional Papers of the British Columbia Provincial Museum No. 13, British Columbia Provincial Museum, Victoria, B.C.

[34] Weir SK (2015) Ovulation synchrony as an adaptive response to egg cannibalism in a seabird colony. Honors thesis, Andrews University. Retrieved from http://digitalcommons.andrews.edu/honors/120/